Published in final edited form as:
Demogr Res. ; 30: 1367–1396. doi:10.4054/DemRes.2014.30.48.

Why do lifespan variability trends for the young and old diverge? A perturbation analysis

Michal Engelman[1], **Hal Caswell**[2], and **Emily M. Agree**[3]

Michal Engelman: mengelman@ssc.wisc.edu

[1]Department of Sociology and Center for Demography and Ecology, University of Wisconsin-Madison, USA

[2]Institute for Biodiversity and Ecosystem Dynamics, University of Amsterdam, Netherlands. Biology Department, Woods Hole Oceanographic Institution, USA

[3]Hopkins Center for Population Aging and Health, Hopkins Population Center, and Department of Sociology, Johns Hopkins University, USA

Abstract

BACKGROUND—Variation in lifespan has followed strikingly different trends for the young and old: while total lifespan variability has decreased as life expectancy at birth has risen, the variability conditional on survival to older ages has increased. These diverging trends reflect changes in the underlying demographic parameters determining age-specific mortality.

OBJECTIVE—We ask why the variation in the ages at death after survival to adult ages has followed a different trend than the variation at younger ages, and aim to explain the divergence in terms of the age pattern of historical mortality changes.

METHODS—Using simulations, we show that the empirical trends in lifespan variation are well characterized using the Siler model, which describes the mortality trajectory using functions representing early-life, later-life, and background mortality. We then obtain maximum likelihood estimates of the Siler parameters for Swedish females from 1900 to 2010. We express mortality in terms of a Markov chain model, and apply matrix calculus to compute the sensitivity of age-specific variance trends to the changes in Siler model parameters.

RESULTS—Our analysis quantifies the influence of changing demographic parameters on lifespan variability at all ages, highlighting the influence of declining childhood mortality on the reduction of lifespan variability, and the influence of subsequent improvements in adult survival on the rising variability of lifespans at older ages.

CONCLUSIONS—These findings provide insight into the dynamic relationship between the age pattern of survival improvements and time trends in lifespan variability.

1. Introduction: Divergence in lifespan variability

To understand the demographic transition of the past century and a half, researchers have analyzed the dynamics of mortality declines using both empirical data and mathematical models. While providing insight into the dramatic increase in longevity, these analyses have also occasionally yielded new puzzles. One of these puzzles concerns the trends and age-pattern of variation in lifespan.

For much of human history, mortality rates at all ages were relatively high and the length of human life was highly variable. During the course of the demographic transition, mortality rates declined, life expectancy rose, and the variability of the distribution of lifespans, or ages at death, changed in response. Robine (2001, p.192) identified two stages in the history of lifespan variability. In the first stage, spanning the late nineteenth and early twentieth century "the level of mortality fell… resulting in a very large reduction in the disparities of life spans." The second stage, starting in the 1950s, was one in which "the increase in life expectancy is no longer associated with a reduction in the dispersion of life spans – or with only a very small reduction." A closer examination of variability trends suggests another key, yet overlooked, aspect of this story. In high-longevity populations, survival improvements have taken place at all ages, including the oldest (Wilmoth et al. 2000; Rau et al. 2008), but trends in the variability of the distribution of ages at death have not exhibited a uniform pattern. Variation in the length of life has declined as life expectancy at birth has risen (Fries 1980; Wilmoth and Horiuchi 1999; Cheung et al. 2005), but the variation in lifespan among survivors to older ages (e.g. 65 and above) has increased (Myers and Manton 1984, Engelman et al. 2010).

Variation in lifespan can be measured with a number of indices, all of which are highly correlated across populations and over time (Wilmoth and Horiuchi 1999; van Raalte and Caswell 2013). Here, we measure lifespan variability by s_x, the standard deviation of the age at death, conditional on survival to the index age x. Figure 1 shows that the standard deviation among newborn individuals, measured relative to its initial value, has declined since 1900, as has the variation in the distributions of ages at death conditional on survival to age 10. However, variation in the age at death among survivors to older ages is higher now than it was a century ago, when the challenges of reaching older ages may have fashioned a more highly selected group of survivors. While the figure relies on data for Swedish females to illustrate this pattern, the diverging age-specific trends have been observed for women and men across industrialized nations and appear to be a common feature of the mortality transition in contemporary high-longevity countries (Engelman et al. 2010).

Because the difference in the trends in lifespan variance by age (s_x) is visually striking, substantial, and persistent, it should be accounted for in mortality models and in explanations of population health patterns. Here, our goal is to explain the changes in s_x in terms of historical changes in the age schedule of mortality. We do so by using the Siler model, which describes mortality in terms of early-life, later-life, and background mortality components. We show that the empirical trends in lifespan variation are well characterized using the Siler model, and obtain maximum likelihood estimates of its parameters. By

expressing lifespan variation in terms of a Markov chain model, we are able to apply perturbation analysis (Caswell 2006, 2008, 2010) to quantify the influence of changes in each parameter of the Siler model on variability trends at all ages. This analysis allows us to ask whether and how the pattern of mortality improvement over time differentially influences age-specific lifespan variability (s_x) trends. Our results detail the impact of declining childhood mortality on the reduction of lifespan variability and the impact of improved survival in adulthood on the rising variability of lifespans at older ages.

1.1 From Gompertz to Siler: Mathematical mortality models

The first attempt to describe the life table survival function in mathematical terms is credited (Smith and Keyfitz 1977) to the French mathematician Abraham de Moivre (1725). de Moivre's model provided a reasonable fit to the first empirical life table constructed by Edmund Halley (1692) for the population of Breslau, but its shortcomings included a lower age limit of 12 and an upper limit of 86 for the "extremity of old age."

A century later, the British actuary Benjamin Gompertz (1825) famously modeled the force of mortality as an exponential function:

$$\mu(x)=e^{\alpha+\beta x}, \quad (1)$$

where α describes the overall hazard levels and β is the rate of mortality increase with age. While the Gompertz model provides a good approximation of adult mortality, it cannot capture the declining hazard of mortality in early life (Canudas-Romo and Engelman 2009) or the deceleration in mortality at the oldest ages (Vaupel et al. 1998). It's best suited for modeling deaths in the general age range of 20–80 (Olshansky and Carnes 1997).

After Gompertz, Thorvald Thiele (1871) and Wilhelm Lexis (1878) both argued that a complete description of the age distribution of deaths required three components. Lexis' categories were based on the distribution of ages at death, and included (1) the "normal group," symmetrically distributed around the modal age of adult deaths; (2) infant and child deaths; and (3) premature adolescent and adult deaths that, Lexis surmised, were unrelated to age. The biologists Pearl and Miner (1935) also proposed a three-type clas-sification, based on the shape of the log survival curve and reflecting constant, increasing, or decreasing resistance to mortality over time.

Following the demographic tradition of three-part mortality modeling, Siler (1979) developed a model with three competing components that together shape the pattern of mortality in animal populations: (1) a hazard that decreases from birth onward as the animal matures and adjusts to its environment (akin to Lexis' second component and Pearl and Miner's "increased resistance" typology); (2) a constant hazard, reflecting a set of age-independent risks present in the "background" (paralleling Pearl and Miner's constant resistance pattern); and (3) a hazard that increases with age to reflect the growing risk of death (and encapsulating the deaths that Lexis characterized as "normal" and Pearl and Miner viewed as a function of decreased resistance to mortality):

$$\mu(x)=e^{\alpha_1-\beta_1 x}+e^{\alpha_2+\beta_2 x}+e^{\alpha_3}. \quad (2)$$

Each Siler component could affect mortality across the full age range. Their additive combination creates a bathtub-shaped age pattern (see Figure 2), with a mortality hazard trajectory that decreases in early life, remains relatively flat between later childhood and young adulthood, and then increases monotonically at older ages.

Contemporary demographers (e.g. Canudas-Romo and Schoen 2005, Goldstein and Wachter 2006) have applied the Siler model to human populations. While the Siler model cannot account for the deceleration in older ages, nor the “hump” (frequently attributed to accidental mortality) in early adulthood, it fits as well or better than most other models to human mortality data across the full age range (Gage and Dyke 1986, Gage and Mode 1993) and is consistent with biological interpretations based on age-specific causes of death (Gage 1991). The Siler model has also been used as a model life table in studies of the demography of primates and marine mammals (Barlow and Boveng 1991, Gage 1998).

1.2 Do mortality models capture variability?

The evaluation of mortality models has centered on their capacity to characterize the change in mortality hazards by age and over time (Keyfitz 1984), focusing on death rates (e.g. Ryder 1975) and on central tendency measures, such as the mean and modal age at death (e.g. Pollard 1991, Thatcher et al. 1998, Kannisto 2001, Canudas-Romo 2008). However, attention to the empirical trends in variability has been growing (Wilmoth and Horiuchi 1999; Edwards and Tuljapurkar 2005; Smits and Monden 2009; Engelman et al. 2010; van Raalte et al. 2011; Brown et al. 2012), and this key aspect of mortality change should be reflected in models used to analyze and project population trends.

Because the Gompertz model focuses exclusively on adult mortality (see Tuljapurkar and Edwards 2011 for an analysis of variability in adult lifespans under the Gompertz model), it cannot capture the diverging trends in variability for the young and old. The Siler model separates child, adult, and background mortality, and thus can capture the contribution of these components to the diverging age-pattern of the trends in lifespan variation that characterize historical mortality transitions in high-longevity populations. (See Appendix A for simulations investigating the extent to which the Gompertz and Siler models are able to depict the growing variability in longevity conditional on survival to older ages, even while characterizing the declining variability in the overall lifespan distribution.) The Siler model can represent a wide array of mortality change scenarios, including the historical patterns that saw child mortality decline before adult mortality. It is thus particularly well-suited for exploring the diverging trends in lifespan variability for the young and old. Below, we focus on quantifying the influence of each Siler model parameter on age-specific variability trends, and show how declining childhood mortality reduced lifespan variability while later improvements in adult survival increased the variability of lifespans at older ages.

2. Data and methods

In this paper, matrices are denoted by boldface upper case symbols (e.g., **P**) and vectors by boldface lower case symbols (e.g., $\boldsymbol{\eta}$). All vectors are column vectors by default; $\boldsymbol{\eta}^{\top}$ denotes the transpose of $\boldsymbol{\eta}$. The identity matrix is **I**, and **1** is a vector of ones. The vector operator creates a vector from a matrix by stacking the columns of the matrix on top of each other. The symbol $\bigcirc$ denotes the Hadamard, or element-by-element product of two matrices, while $\otimes$ denotes the Kronecker product.

We used data from he Human Mortality Database (HMD 2013), which contains detailed time series of mortality data and life tables for populations with virtually complete registration and census data. To examine the changing distribution of lifespan during periods of notable mortality transitions, we analyzed data for females from Sweden – the nation with the longest and most reliable time-series of vital statistics. Using life tables for every year during the period between 1900 and 2010, we obtained maximum-likelihood estimates for the five parameters of the Siler model (see Appendix B for the estimation procedure).

Trends in lifespan variability are the result of changes in the underlying demographic parameters determining age-specific mortality. The Siler model describes mortality hazards using scale parameters (a_1, a_2, a_3) describing the level of mortality at younger ages, older ages, and overall, as well as age-trend parameters (β_1, β_2) describing the slope of the hazard trajectory at younger ages and older ages. The analysis below describes the sensitivity of lifespan variability (measured via s_x the standard deviation of the distribution of lifespans beyond a given age x) to changes in the Siler model parameters.

Defined broadly, sensitivity analysis quantifies the change in an outcome variable in response to a change in one or more variables on which the outcome depends (Caswell 1978). In demography, perturbation analysis has been used to describe the sensitivity of population growth rates to changes in the environment or in vital rates (Demetrius 1969; Keyfitz 1971; Goodman 1971; Caswell 1978, 2010), and the sensitivity of life expectancy to changes in age-specific mortality rates (Keyfitz 1971, 1977; Pollard 1982; Vaupel 1986; Keyfitz and Caswell 2005; Caswell 2006, 2009; Wrycza and Baudisch 2012).

Because trends in lifespan variability depend on the changing distribution of mortality, sensitivity analysis offers an appealing way to quantify the influence of each component of the Siler model on lifespan variability patterns across both age and time. We will do this by describing longevity with an absorbing Markov chain model and applying newly-developed matrix calculus methods (e.g., Caswell 2006, 2008, 2009, 2010; van Raalte and Caswell 2013). The Markov chain formulation assumes that individuals move through a set of transient states – in this case, age classes – over their life cycle and eventually die, or, in Markov chain terminology, enter an absorbing state in which they remain thereafter. Since absorption (i.e., death) is eventually certain for all individuals, analyses of conditional longevity measures are analogous to investigating how long it takes until absorption occurs and what the distribution of absorption times is, given different initial states or ages. Matrix calculus provides a notational framework that permits the consistent differentiation of functions of scalar, vector or matrix arguments.

We represent age-specific mortality rates by a vector $\boldsymbol{\mu}$. The vector of age-specific survival probabilities is

$$\mathbf{p}=e^{-\boldsymbol{\mu}} \quad (3)$$

where the exponential is applied element-wise. Letting $\mathbf{x} = (0, \cdots, 110)^{\top}$, then the mortality vector $\boldsymbol{\mu}$ is a function of the parameters of the Siler model

$$\boldsymbol{\mu}=e^{\alpha_1}e^{-\beta_1\mathbf{x}}+e^{\alpha_2}e^{\beta_2\mathbf{x}}+e^{\alpha_3} \quad (4)$$

The Markov chain transition matrix representing the probabilities of survival and mortality from one age to the next can be written as

$$\mathbf{P}=\left(\begin{array}{c|c}\mathbf{U} & \mathbf{0}\\ \hline \mathbf{M} & \mathbf{I}\end{array}\right), \quad (5)$$

where **M** is a matrix of mortality rates and **I** is an identity matrix that assures that dead individuals remain in their absorbing state. If only a single absorbing state is identified, then **M** is a row vector, and **I** is the scalar 1. The matrix **U** is the transition matrix among the living states; it has the survival vector **p** on the subdiagonal and zeros elsewhere,

$$\mathbf{U}=\begin{pmatrix} 0 & \cdots & \cdots & 0\\ p_1 & & & \\ & \ddots & & \\ & & p_{110} & 0\end{pmatrix}. \quad (6)$$

The last diagonal entry of **U** is zero, as no one survives beyond the final (absorbing) age category in the life table.

Within this framework, the longevity of an individual in age class *x* is the time remaining until the individual enters the absorbing state. The statistics of longevity are calculated from the fundamental matrix $\mathbf{N} = (\mathbf{I} - \mathbf{U})^{-1}$, whose (*i*, *j*) entry is the mean number of visits to state *i* conditional on survival to state *j*. The vectors representing the expected lifespan (η, or time until death), its variance, and the standard deviation are:

$$\overline{\boldsymbol{\eta}}^{\top}=\mathbf{1}^{\top}\mathbf{N} \quad (7)$$

$$V(\boldsymbol{\eta})^{\top}=\mathbf{1}^{\top}\mathbf{N}\,(2\mathbf{N}-\mathbf{I})-\overline{\boldsymbol{\eta}}^{\top}\circ\overline{\boldsymbol{\eta}}^{\top} \quad (8)$$

$$\mathbf{s}=\sqrt{V(\boldsymbol{\eta})} \quad (9)$$

where **1** is a column vector of ones, $\circ$ denotes element-by-element multiplication, and the square root is applied element-wise (for derivations in a demographic context, see Caswell 2006, 2009, 2010).

Our goal is a sensitivity analysis that will provide the derivatives of **s** (the vector of standard deviations of lifespans after successive index ages) with respect to the parameters of the Siler model, given by the vector $\boldsymbol{\theta} = (\alpha_1, \beta_1, \alpha_2, \beta_2, \alpha_3)^\top$. Previous sensitivity analyses have focused on perturbations of mortality at a single specified age (Zhang and Vaupel 2009; Caswell 2010, 2013; van Raalte and Caswell 2013; Gillespie et al. 2014). These studies have shown, for many measures of variability, the existence of a critical age: before this age, the sensitivity of variability to mortality is positive (i.e declines in mortality contract variability); after it, the sensitivity is negative (i.e. mortality declines expand variability). Mortality models such as the Siler model provide parameters that influence the entire age pattern of mortality. This frees us from considering only single ages. Perturbations in α_1 and β_1 (the childhood mortality parameters) have their largest effects at ages before the critical age, whereas α_2 and β_2 (the adult mortality parameters) affect mortality more at ages past the critical age.

Our methods rely on matrix calculus, as used by Caswell (2006, 2008, 2013, van Raalte and Caswell 2013). The first step is to differentiate the variance $V(\boldsymbol{\eta})$ with respect to the matrix **U**, and then apply the chain rule successively to link **U** with the Siler hazard model, obtaining

$$\frac{dV(\boldsymbol{\eta})}{d\boldsymbol{\theta}^\top} = \left[2(\mathbf{N}^\top \otimes \mathbf{1}^\top) + 2(\mathbf{I} \otimes \mathbf{1}^\top \mathbf{N}) - (\mathbf{I} \otimes \mathbf{1}^\top) - 2\left[\operatorname{diag}(\overline{\boldsymbol{\eta}})\right](\mathbf{I} \otimes \mathbf{1}^\top)\right] (\mathbf{N}^\top \otimes \mathbf{N}) \frac{d\operatorname{vec}\mathbf{U}}{d\boldsymbol{\theta}^\top}. \quad (10)$$

The derivative of the vector **s** of standard deviations of lifespan lengths is then

$$\frac{d\mathbf{s}}{d\boldsymbol{\theta}^\top} = \frac{1}{2}\operatorname{diag}(\mathbf{s})^{-1} \frac{dV(\boldsymbol{\eta})}{d\boldsymbol{\theta}^\top}. \quad (11)$$

The final step in the derivation requires the derivatives of the transition matrix **U**, given in (6), with respect to the Siler model parameters. These are obtained by writing

$$d\operatorname{vec}\mathbf{U} = \operatorname{diag}(\operatorname{vec}\mathbf{J})(\mathbf{1} \otimes \mathbf{I}) d\mathbf{p}, \quad (12)$$

where **J** is a square matrix, with ones on the sub-diagonal and zeros elsewhere, and then noting that

$$d\mathbf{p} = -\operatorname{diag}(\mathbf{p}) d\boldsymbol{\mu}. \quad (13)$$

Combining the results give the derivative with respect to the Siler parameter vector as *d*vec **U**

$$\frac{d\mathrm{vec}\,\mathbf{U}}{d\boldsymbol{\theta}^{\top}}=-\mathrm{diag}\,(\mathrm{vec}\,\mathbf{J})(\mathbf{1}\otimes\mathbf{I})\mathrm{diag}\,(\mathbf{p})\frac{d\boldsymbol{\mu}}{d\boldsymbol{\theta}}. \quad (14)$$

The derivative of the mortality vector $\boldsymbol{\mu}$ with respect to the Siler model parameters is obtained by rewriting the Siler model (4) as

$$\boldsymbol{\mu}(x)=e^{\mathbf{w}_1}+e^{\mathbf{w}_2}+e^{\mathbf{w}_3}, \quad (15)$$

with the corresponding derivatives:

$$d\boldsymbol{\mu}=\mathrm{diag}\,(e^{\mathbf{w}_1})\,d\mathbf{w}_1+\mathrm{diag}\,(e^{\mathbf{w}_2})\,d\mathbf{w}_2+\mathrm{diag}\,(e^{\mathbf{w}_3})\,d\mathbf{w}_3, \quad (16)$$

where

$$\begin{aligned} d\mathbf{w}_1&=\mathbf{1}d\alpha_1-\mathbf{x}(d\beta_1)\\ d\mathbf{w}_2&=\mathbf{1}d\alpha_2+\mathbf{x}(d\beta_2)\\ d\mathbf{w}_3&=\mathbf{1}d\alpha_3. \end{aligned} \quad (17)$$

This perturbation method combines the sensitivity of the Siler mortality components in (17), the sensitivity of the transition matrix **U** to mortality in (14), and the sensitivity of **s** to the transition matrix **U** in (11) and (10). The analyses allow us to determine and quantify the sensitivity of our outcome of interest (the standard deviation of the distribution of lifespans beyond any given age) to unit changes in each of the five Siler model parameters. The results below demonstrate how the pattern of mortality improvement over time – as reflected in changes in the Siler model parameters – differentially affects lifespan variability conditional on survival to younger and older ages.

3. Results

Figure 3 presents maximum likelihood estimates for the Siler model parameters from 1900–2010. Each parameter is represented in its own scale, to facilitate the analysis of trends. The a parameters, representing the overall levels of child, adult, and background mortality, decline over time, although a_2 (the adult parameter) first increased slightly between 1900–1930 before declining. All three a parameters are negative, with a_2 always less than a_1 and a_3. Both β slope parameters are positive, with β_1 more than an order of magnitude larger than β_2. The value of β_1, which represents the rate of decline in childhood mortality with age, increased dramatically from 1900–1940, and then remained roughly constant — a result consistent with the known improvements in infant survival. The trend in β_2, which represents the rate of increase in adult mortality with age, mirrors the a_2 trend: first declining between 1900–1930, and then increasing during the latter part of the twentieth century, although the overall variation is small. Thus the slope of the adult hazard trajectory has grown slightly steeper since 1930, even as age-specific mortality hazards have declined, with mortality being increasingly compressed into the latter part of life. Overall, infant and childhood mortality declined earlier in the century, and adult survival improvement followed in subsequent decades.

Figure 4 presents the sensitivity of s_x (the standard deviation of lifespan beyond age x) to changes in each Siler parameter for five selected years between 1900 and 2010. Regardless of age or time,

$$\frac{ds_x}{d\alpha_1} > 0 \quad (18)$$

$$\frac{ds_x}{d\alpha_2} < 0 \quad (19)$$

$$\frac{ds_x}{d\alpha_3} > 0 \quad (20)$$

$$\frac{ds_x}{d\beta_1} < 0 \quad (21)$$

$$\frac{ds_x}{d\beta_2} < 0. \quad (22)$$

That is, the variability in lifespan is increased by higher baseline infant mortality and reduced by a faster rate of decay of that mortality component with age, because these changes primarily affect mortality (positively and negatively, respectively) before the critical age. Conversely, lifespan variability is reduced by higher baseline old age mortality and by increases in the rate of late-life mortality; these changes have their biggest effects at old ages, past the critical age. Finally, variability in lifespan is increased by increases in the age-independent component of mortality. The standard deviation of remaining lifespan at all ages is most sensitive to changes in the value of β_2, the slope parameter for adult mortality. Note that the greater impact of α_1 and β_1 at young ages, and of α_3 and β_3 at older ages means that these results reflect an integration of effects on both sides of the critical age.

The sensitivities of s_x to the parameters representing infant mortality mirror each other, with α_1 positive, β_1 negative, and both approaching zero with increasing age and over time. The mirrored trajectories reflect the two parameters' complementarity and interdependence in determining the hazard of mortality in early childhood. Notably, while in 1900 the absolute magnitude of the sensitivities to α_1 and β_1 were relatively high, and each parameter's visible impact extended up to age 5, by later years the sensitivity declined markedly, and the two parameters' influence was confined to the first year of life. As one might expect, the two childhood parameters only affect s_x for ages that include mortality in early life, but their sensitivities approach zero as age increases. A similar pattern of decline with age and over time is apparent for the sensitivity to α_3, the parameter determining background or overall mortality level. The sensitivity to α_3 at all ages has declined over time, but remains appreciable at younger ages and up to midlife. Up through the reproductive ages, s_x is more sensitive to changes in α_3 than to changes in α_1, indicating the importance of overall mortality conditions to the pattern of variability in lifespans.

In contrast to the diminishing influence of the other parameters across the life course, the adult mortality parameters α_2 and β_2 remain influential across the full age spectrum. The sensitivity of s_x to both parameters is negative at all ages, implying that an increase in either the overall level or rate of increase of adult mortality would reduce variability, and, conversely, that improved survival in adulthood will increase age-specific variation. The sensitivity of s_x to β_2 is substantially greater than its sensitivity to all other parameters – nearly two orders of magnitude bigger than the sensitivity to β_1 or α_2.

The age-pattern of the two adult mortality parameters' influence on the variability of the lifespan distribution differs substantially from that of the other parameters (see Figure 4). In 1900, the sensitivity of s_x to changes in both α_2 and β_2 was strongly negative for measures conditional on survival to young ages, with lower absolute sensitivity at older ages. For both parameters, the change in sensitivity with age was more marked at older ages than it was at younger ages, with a plateau between (roughly) ages 50 and 70. Throughout the 20th century, the sensitivity to both parameters declined in absolute magnitude at younger ages, while the sensitivity at older ages increased slightly. By the second half of the twentieth century, the resulting age trajectory featured a slight decline in sensitivity from birth up to age 50, relatively more absolute sensitivity for measures conditional on survival to age 50–75, and finally a steep reversal and decreased absolute sensitivity for measures conditional on survival to older ages.

For a more detailed longitudinal perspective on the relationship between the Siler parameters and conditional variability for selected ages, Figure 5 presents the trends in the sensitivity of the standard deviation of the lifespan distribution for survivors to selected ages (0, 10, 50, and 75) to each Siler model parameter. The sensitivities of s_0 to each parameter have changed dramatically over the course of the twentieth century. For example, while the childhood mortality parameters α_1 and β_1 were quite influential for s_0 in 1900, its sensitivity to them declined steeply after that. Another steep decline, followed by stable lower rate, is apparent in the sensitivity of s_0 to α_3, the background mortality component. The sensitivity of s_0 to the two adult mortality parameters, α_2 and β_2, also shows two distinct phases: it rapidly moves towards less negative values during the first part of the century, and then stabilizes (or continues to decline very slowly) during the latter part of the time series. Trends for the sensitivity of s_{10} to the same parameters follow a similar pattern, consistent with the reductions in early-life mortality which took place in the first half of the twentieth century.

Figure 5 also indicates that the standard deviations at older ages (s_{50} and s_{75}) are insensitive to the childhood mortality parameters; s_{50} (but not s_{75}) shows slight responsiveness to α_3 early in the twentieth century, but this sensitivity wanes over the decades. The main contrast between the two indices is apparent in their sensitivities to the adult mortality parameters α_2 and β_2, which were similar in 1900, but have diverged substantially since. The relative stability in the sensitivity of s_{75} to the two parameters over time stands in contrast to the declining sensitivity in measures conditional on survival to younger ages: while s_{75} was relatively *less* sensitive to α_2 and β_2 in the first part of the twentieth century than s_0, s_{10}, and s_{50}, the mid-century cross-over has resulted in a *greater* contemporary sensitivity of s_{75} to α_2 and β_2, relative to variability measures conditional on survival to younger ages. Thus, the

influence of the Siler model's adult parameters on longevity variation is apparent at increasingly older index ages.

In summary, the sensitivity patterns shed some light on the divergent trends in longevity variation. The standard deviation for younger ages decreases over time because its sensitivities to a_1 and a_3 are positive, and those parameter values have decreased over the course of the last century's demographic transition. The sensitivities to the two β parameters are negative and β_1 and β_2 have both increased, likewise reducing the standard deviation for survivors to younger ages. At the older ages, the sensitivity of s_x to the two adult mortality parameters is negative, a_2 has decreased and β_2 has increased only slightly, leading in combination to a trend of increased variability. Sensitivity to the childhood and background parameters a_1, β_1, and a_3 approaches zero at older ages, so these parameters do not exercise an influence on the pattern of variability at older ages. Finally, s_x is stable in the immediate post-reproductive years because of the countervailing effects of the positive sensitivity to a_3 and the negative sensitivity to adult mortality parameters which are operating in conjunction to shape variability patterns at these younger-old ages.

4. Discussion

A focus on variability requires going beyond measures of central tendency to characterize the pattern of mortality across the full range of ages, yet previous evaluations of mathematical mortality models have rarely considered their capacity to accurately represent age differences in lifespan variability trends. Our simulations (see Appendix A) showed that while the widely-used Gompertz model suggests a link between improved survival and increased lifespan variation in adulthood, it cannot account for the diverging trends for the young and old that are a key feature of the historical mortality transition in high-longevity countries. The three-component Siler model, however, can produce a pattern of compression in lifespan variability accompanied by increasing variability conditional on survival to older ages. Furthermore, the time trends in the Siler model parameters highlight the earlier reduction in early-life mortality and the subsequent reduction in adult mortality, another notable characteristic of the demographic transition during the nineteenth and twentieth centuries.

The perturbation analysis of the Siler model indicates that the conspicuously diverging patterns of lifespan variation by age are due to the differential impact of mortality reduction in childhood and adulthood on the distribution of ages at death. These dynamics across time and age are essential for understanding the patterns of change in life expectancy as well as in the variability of lifespans. Our analysis adds to previous work on mortality change and lifespan variability by examining the effects of each Siler parameter on mortality at every age, and by precisely quantifying the extent to which lifespan variability is increased or decreased by changes to specific components of the overall mortality trajectory.

Previous research has shown that lives saved at younger ages reduce lifespan disparity, while lives saved at older ages increase it (Zhang and Vaupel 2009; van Raalte and Caswell 2013; Gillespie et al. 2014), with the threshold demarcating early and late ages changing in response to changes in the mortality schedule and the historical contingencies that shape it.

Our results likewise indicate that early and late deaths have different implications for the variability of lifespan conditional on survival to successive ages. Perturbation analysis enabled us to quantify this relationship, showing the differential responses of variability measure conditional on survival to younger and older ages to the parameters defining the course of child, adult, and background mortality levels. In particular, we showed that lifespan variability decreases for younger ages because of its sensitivity to the childhood mortality parameters, and that lifespan variability at older ages has increased because its sensitivity to the decline in adult mortality is in fact negative.

The Siler parameters that primarily define the early childhood component of mortality (α_1 and β_1) influenced lifespan variability substantially when early-life mortality was still high at the turn of the twentieth century, but this influence waned as the absolute value of the parameters shifted to reflect declining levels of mortality in infancy and the childhood years. Sweden's current extremely low level of childhood mortality is thus apparent both in the Siler childhood parameter values and in the declining sensitivity of lifespan variability at all ages (even the youngest) to these parameters over time. A similar pattern holds for the background-mortality element (α_3).

In contrast, the two parameters that define adult mortality (α_2 and β_2) exercised an increasingly noticeable effect on mortality starting in the 1930s, and remained influential throughout the latter half of the twentieth century and into the twenty-first. Variability indices conditional on survival into older ages have maintained and even somewhat increased their sensitivity to these parameters. The parameter trends reflect the sustained decline in mortality at increasingly older ages (Vaupel 2010), while the sensitivity trends reflects an inverse relationship between improved old-age survival and the variability of lifespans for survivors into later life.

Notably, the expansion of lifespan variability at older ages takes place despite the fact that deaths are being concentrated into older ages. While the classic description of mortality compression (Fries 1980) predicts that lifespan variability will decline as life expectancy rises, this decline in variability doesn't materialize at older ages because, as we show, the relationship between mortality rates and lifespan variability is negative at those ages. While the data leave no doubt that deaths are indeed being delayed into increasingly older ages, our analysis shows that the implications of such changes for lifespan variability patterns are not pre-determined, but rather depend in intricate ways on the specific pattern of mortality change by age and over time.

The longitudinal nature of our analysis further highlights the impact of the temporal pattern of mortality change (i.e. an initial decline in childhood mortality followed by a decline in adult mortality some decades later) on the differential trends in lifespan variability at younger and older ages. Mortality has declined at all ages, but not at the same time or to the same extent. For the successive cohorts aging through the dramatic population changes of the twentieth century, survival has improved at all ages, but more so in early life than in adulthood. At the same time, each successive cohort is reaching older ages with added benefits of lower mortality (and likely better health) throughout the life course, suggesting that the period trends we describe here may also be explained by cohort effects and changing

distributions of health and vulnerability to mortality within cohorts (see Engelman et al. 2013 for a more detailed analysis of this possibility).

It is important to remember that while the parameters of the Siler model are notable for their meaningful interpretations, inference based on individual parameter values should be undertaken cautiously, due to the high correlation between model parameters (see Hartmann 1987) and the co-determination of best-fitting parameter values by our maximum likelihood estimation procedure. This interdependence is particularly notable in the case of parameter pairs (e.g. a_1 and β_1 or a_2 and β_2) that jointly describe the level and age slope of particular mortality components. Overall, however, the trends we identify are consistent with the changes that took place over the course of the demographic and epi-demiological transitions of the twentieth century.

Perturbation analysis has enabled a more detailed quantification of the influence of changing demographic parameters on the pattern of lifespan variability at all ages, highlighting the impact of declining childhood mortality on the reduction of lifespan variability, and the impact of later improvements in adult survival on the rising variability of lifespans at older ages. Future research may further draw on the Siler model and perturbation methods to decompose mortality change, characterizing the relative contributions of changes in background, infant, adult, and old-age mortality to the demographic transformations of the past century and half, as well as projecting the components of future changes with greater precision.

Acknowledgments

Michal Engelman acknowledges support from the Sommer Scholars program at the Johns Hopkins Bloomberg School of Public Health and from the Center for Demography and Ecology (NICHD R24 HD047873) and Center for Demography of Health and Aging (NIA P30 AG17266) at the University of Wisconsin-Madison. Hal Caswell acknowledges support from the Alexander von Humboldt Foundation, National Science Foundation (MMS-1156378 and DEB-1257545), and the European Research Council (Advanced Grant 322989), as well as the hospitality of the Max Planck Institute for Demographic Research. We thank John Tillinghast for invaluable assistance with Matlab-to-R translations and Karen Bandeen-Roche, Vladimir Canudas-Romo, and the anonymous reviewers for helpful comments on earlier drafts of the manuscript.

References

Barlow J, Boveng P. Modeling age-specific mortality for marine mammal populations. Marine Mammal Science. 1991; 7(1):50–65.10.1111/j.1748-7692.1991.tb00550.x

Brown DC, Hayward MD, Montez J, Hummer R, Chiu CT, Hidajat M. The significance of education for mortality compression in the united states. Demography. 2012; 49(3):819–840.10.1007/s13524-012-0104-1 [PubMed: 22556045]

Canudas-Romo V. The modal age at death and the shifting mortality hypothesis. Demographic Research. 2008; 19(30):1179–1204.10.4054/DemRes.2008.19.30

Canudas-Romo V, Engelman M. Maximum life expectancies: revisiting the best practice trends. Genus. 2009; 65(1):59–79.

Canudas-Romo V, Schoen R. Age-specific contributions to changes in the period and cohort life expectancy. Demographic Research. 2005; 13(3):63–82.10.4054/DemRes.2005.13.3

Caswell H. A general formula for the sensitivity of population growth rate to changes in life history parameters. Theoretical Population Biology. 1978; 14(2):215–230.10.1016/0040-5809(78)90025-4 [PubMed: 371054]

Caswell, H. Applications of markov chains in demography. In: Langville, A.; Stewart, W., editors. MAM 2006: An International Conference to Celebrate the 150th Anniversary of the Birth of AA Markov. Raleigh, North Carolina; Boson Books: 2006. p. 319-334.

Caswell H. Perturbation analysis of nonlinear matrix population models. Demographic Research. 2008; 18(3):59–116.10.4054/DemRes.2008.18.3

Caswell H. Stage, age and individual stochasticity in demography. Oikos. 2009; 118(12):1763–1782.10.1111/j.1600-0706.2009.17620.x

Caswell, H. Perturbation analysis of longevity using matrix calculus. Paper presented at the 2010 meeting of the Population Association of America; Dallas, Texas. 2010.

Caswell H. Sensitivity analysis of discrete markov chains via matrix calculus. Linear Algebra and its Applications. 2013; 438(4):1727–1745.10.1016/j.laa.2011.07.046

Cheung SLK, Robine JM, Tu EJC, Caselli G. Three dimensions of the survival curve: Horizontalization, verticalization, and longevity extension. Demography. 2005; 42(2):243–258. [PubMed: 15986985]

Chiang, C. The life table and its applications. Malabar: Krieger Pub. Co; 1984.

de Moivre, A. Annuities Upon Lives: Or, the Valuation of Annuities Upon Any Number of Lives; as Also, of Reversions. London: W. P. and sold by Francis Fayram and Benj. Motte; and W. Pearson; 1725.

Demetrius L. The sensitivity of population growth rate to pertubations in the life cycle components. Mathematical Biosciences. 1969; 4(1âĂŞ2):129–136.10.1016/0025-5564(69)90009-1

Edwards RD, Tuljapurkar S. Inequality in life spans and a new perspective on mortality convergence across industrialized countries. Population and Development Review. 2005; 31(4):645–674.10.1111/j.1728-4457.2005.00092.x

Engelman, M.; Canudas-Romo, V.; Agree, E. Frailty in transition: Vulnerability and variation in aging populations. Madison, Wisconsin: Center for Demography and Ecology; 2013. (CDE Working Paper No. 2013-10)

Engelman M, Canudas-Romo V, Agree EM. The implications of increased survivorship for mortality variation in aging populations. Population and Development Review. 2010; 36(3):511–539.10.1111/j.1728-4457.2010.00344.x [PubMed: 20882704]

Fries JF. Aging, natural death, and the compression of morbidity. New England Journal of Medicine. 1980; 303(3):130–135.10.1056/NEJM198007173030304 [PubMed: 7383070]

Gage TB. Causes of death and the components of mortality: Testing the biological interpretations of a competing hazards model. American Journal of Human Biology. 1991; 3(3):289–300.10.1002/ajhb.1310030308

Gage TB. The comparative demography of primates: With some comments on the evolution of life histories. Annual Review of Anthropology. 1998; 27(1):197–221.10.1146/annurev.anthro.27.1.197

Gage TB, Dyke B. Parameterizing abridged mortality tables: The siler three-component hazard model. Human Biology. 1986; 58(2):275–291. [PubMed: 3710467]

Gage TB, Mode C. Some laws of mortality: How well do they fit? Human Biology. 1993; 65(3):445–461. [PubMed: 8319943]

Gillespie D, Trotter MV, Tuljapurkar SD. Divergence in age-patterns of mortality change drives international divergence in lifespan inequality. Demography. 2014 in press.

Goldstein JR, Wachter KW. Relationships between period and cohort life expectancy: Gaps and lags. Population Studies. 2006; 60(3):257–269.10.1080/00324720600895876 [PubMed: 17060053]

Gompertz B. On the nature of the function expressive of the law of human mortality, and on a new mode of determining the value of life contingencies. Philosophical Transactions of the Royal Society of London. 1825; 115:513–583.10.1098/rstl.1825.0026

Goodman LA. On the sensitivity of the intrinsic growth rate to changes in the age-specific birth and death rates. Theoretical Population Biology. 1971; 2(3):339–354.10.1016/0040-5809(71)90025-6

Halley E. An estimate of the degrees of the mortality of mankind. Philosophical Transactions. 1692; 196(3):596–610. 654–656.

Hartmann M. Past and recent attempts to model mortality at all ages. Journal of Official Statistics. 1987; 3(1):19–36. [PubMed: 12342229]

HMD. The human mortality database. [electronic resource]. University of Cal-ifornia; Berkeley: Max Planck Institute for Demographic Research; Germany: 2013. www.mortality.org

Kannisto V. Mode and dispersion of the length of life. Population: An English Selection. 2001; 13(1): 159–171.

Keyfitz, N. Applied mathematical demography. New York: Wiley; 1977.

Keyfitz, N.; Caswell, H. Applied mathematical demography. 3. New York: Springer-Verlag; 2005.

Keyfitz N. Linkages of intrinsic to age-specific rates. Journal of the American Statistical Association. 1971; 66(334):275–281.

Keyfitz, N. In: Vallin, J.; Pollard, J.; Heligman, L., editors. Choice of function for mortality analysis: Effective forecasting depends on a minimum parameter representation; Methodologies for the collection and analysis of mortality data:proceedings of a seminar; Dakar, Senegal. July 7–10, 1981; Liege, Belgium: Ordina Editions; 1984. p. 225-243.

Lexis W. Sur la duree normale de la vie humaine et sur la theorie de la stabilite des rapports statistiques. Annales de demographie internationale. 1878; 11(2):447–462.

Myers GC, Manton KG. Compression of mortality: Myth or reality? The Gerontologist. 1984; 24(4): 346–353. [PubMed: 6479647]

Nash JC, Varadhan R. Unifying Optimization Algorithms to Aid Software System Users: optimx for R. Journal of Statistical Software. 2011; 43(9):1–14. [PubMed: 22003319]

Olshansky SJ, Carnes BA. Ever since gompertz. Demography. 1997; 34(1):1–15. [PubMed: 9074828]

Pearl R, Miner J. Experimental studies on the duration of life. xiv. the comparative mortality of certain lower organisms. Quarterly Review of Biology. 1935; 10(1):60–79.

Pollard JH. The expectation of life and its relationship to mortality. Journal of the Institute of Actuaries. 1982; 109:225–240.10.1017/S0020268100036258

Pollard JH. Fun with Gompertz. Genus. 1991; 47(1/2):1–20. [PubMed: 12284816]

Rau R, Soroko E, Jasilionis D, Vaupel JW. Continued reductions in mortality at advanced ages. Population and Development Review. 2008; 34(4):747–768.10.1111/j.1728-4457.2008.00249.x

Robine JM. Redefining the stages of the epidemiological transition by a study of the dispersion of life spans: The case of france. Population: An English Selection. 2001; 13(1):173–193.

Ryder NB. Notes on stationary populations. Population Index. 1975; 41(1):3–28.10.2307/2734140

Siler W. A competing-risk model for animal mortality. Ecology. 1979; 60(4):750–757.10.2307/1936612

Smith, D.; Keyfitz, N. Mathematical Demography: Selected Papers. New York: Springer Verlag; 1977.

Smits J, Monden C. Length of life inequality around the globe. Social Science and Medicine. 2009; 68(6):1114–1123. [PubMed: 19176269]

Thatcher, A.; Kannisto, V.; Vaupel, J. Odense Monographs on Population Aging Series. Odense, Denmark: Odense University Press; 1998. The Force of Mortality at Ages 80 to 120.

Thiele TN. On a mathematical formula to express the rate of mortality throughout the whole of life. Journal of the Institute of Actuaries and Assurance Magazine. 1871; 16(5):313–329.

Tuljapurkar S, Edwards RD. Variance in death and its implications for modeling and forecasting mortality. Demographic Research. 2011; 24(21):497–526.10.4054/DemRes.2011.24.21 [PubMed: 25328439]

van Raalte A, Caswell H. Perturbation analysis of indices of lifespan variability. Demography. 2013; 50(5):1615–1640.10.1007/s13524-013-0223-3 [PubMed: 24043610]

van Raalte AA, Kunst AE, Deboosere P, Leinsalu M, Lundberg O, Martikainen P, Strand BH, Artnik B, Wojtyniak B, Mackenbach JP. More variation in lifespan in lower educated groups: evidence from 10 european countries. International Journal of Epidemiology. 2011; 40(6):1703–1714.10.1093/ije/dyr146 [PubMed: 22268238]

Vaupel JW, Carey JR, Christensen K, Johnson TE, Yashin AI, Holm NV, Ia-chine IA, Kannisto V, Khazaeli AA, Liedo P, Longo VD, Zeng Y, Manton KG, Curtsinger JW. Biodemographic trajectories of longevity. Science. 1998; 280(5365):855–860.10.1126/science.280.5365.855 [PubMed: 9599158]

Vaupel J. How change in age-specific mortality affects life expectancy. Population Studies. 1986; 40:147–157. [PubMed: 11611920]

Vaupel J. Biodemography of human ageing. Nature. 2010; 464(7288):536–542.10.1038/nature08984 [PubMed: 20336136]

Wilmoth JR, Deegan LJ, LundstrÃűm H, Horiuchi S. Increase of maximum life-span in sweden, 1861–1999. Science. 2000; 289(5488):2366–2368.10.1126/science.289.5488.2366 [PubMed: 11009426]

Wilmoth JR, Horiuchi S. Rectangularization revisited: Variability of age at death within human populations. Demography. 1999; 36(4):475–495.10.2307/2648085 [PubMed: 10604076]

Wrycza T, Baudisch A. How life expectancy varies with perturbations in age-specific mortality. Demographic Research. 2012; 8(13):365–376.10.4054/DemRes.2012.27.13

Zhang Z, Vaupel JW. The age separating early deaths from late deaths. Demographic Research. 2009; 8(29):721–730.10.4054/DemRes.2009.20.29

Appendix

A Simulations

We simulated the impact of changes over time in mortality rates on the age-pattern of longevity variability using the Gompertz and Siler models. First, using data on Swedish females in 1900, we employed maximum likelihood techniques to obtain estimates of the parameters for each model (see Appendix B for an elaboration of this method). We then simulated a pattern of constant annual change in mortality over time *t* using each model.

For the Gompertz model, the following adaptation was used to represent change in each age-specific mortality hazard:

$$\mu(x,t)=e^{\alpha+\beta x-\rho t}. \quad (23)$$

For the Siler model, we allowed each of the three childhood, adulthood, and background mortality components to have its own change parameter according to the formula:

$$\mu(x)=e^{\alpha_1-\beta_1 x-\rho_c t}+e^{\alpha_2+\beta_2 x-\rho_a t}+e^{\alpha_3-\rho_b t}. \quad (24)$$

By allowing each component to change separately, we imposed no assumptions about the relationships between the three mortality components. Though the rate of change in each component may not in fact be independent from the rates of change in the other two components, the independence assumption is less restrictive than an assigned relationship. Given knowledge of the historical pattern of mortality change, we expected a scenario in which child mortality declined faster than adult mortality to yield the most realistic lifespan variability patterns. Because a background mortality component that is not age-dependent has not been investigated as thoroughly as mortality specific to childhood or adulthood, we paid special attention to its pattern of decline relative to the other two components, and to its influence on the age-pattern of lifespan variability trends.

For simplicity, we assumed the annual change in each parameter value was constant over the simulation time frame. Each ρ parameter was assigned a value of either 0.005, 0.01, or 0.02. These three values were selected to represent a range of relative change scenarios within the

bounds of values that produced a reasonable age-schedule of mortality: i.e. values that generated age-specific mortality probabilities within the (0,1) bounds.

Each model-based change scenario was used to simulate a schedule of mortality decline for 111 years (for comparability with the Swedish data for 1900–2010). For each year, the simulated age-specific mortality hazard measures were used to construct an associated life table (see HMD (2013) for a description of the life table construction method). For each life table, standard deviations were calculated for the complete distribution of ages at death as well as left-truncated or conditional distributions comprising only individuals who survived up to each age age x, (s_x). These conditional age-specific standard deviation measures were divided by their baseline value (i.e. their value in 1900) to obtain period-standardized measures of variability that were uniformly scaled across all ages.

The resulting ratios are equal to 1 if there was no change in the standard deviation for survivors to any given age x since 1900, and the comparison of trends in the age-specific relative deviation measures allow rising and falling patterns to be distinguished on the same scale. The empirical age-specific lifespan variability trends in Figure 1 were then compared to simulated trends produced using the Gompertz and Siler models.

As can be seen in the simulation-based panels in Figure A1, a Gompertz model that includes a term for declines in age-specific mortality over time fails to produce a divergent age-pattern of lifespan variability trends. When the rate of change in the Gompertz model is extremely slow ($\rho = 0.0001$, not shown), there is virtually no change in the relative ratio of standard deviations, while $\rho = 0.005$ leads to a very slight increases in variability at all ages. For $\rho = 0.01$, there is a hint of contracting variation trend at the very oldest ages, the opposite direction from that observed in the empirical plot. As the rate of mortality decline is allowed to increase ($\rho = 0.02$), the apparent pattern is one of an initial period of increased variability followed by a marked decline in lifespan variability at all ages.

Figure A2 depicts analogous simulations that take advantage of the distinct childhood, adult, and background mortality components of the Siler model. Under some scenarios, the three-component model is better able to capture the diverging lifespan variability trends than the Gompertz model. The figure presents cases in which childhood mortality changes faster than adult mortality (consistent with known historical patterns) and the change in background mortality varies from slowest (1) to intermediate (2) and fastest (3). Of the three scenarios, the two in which background mortality changes at a faster pace than either one or both age-specific components are most similar to the empirical plot, though in scenario 3 the s_{10} declines more dramatically than s_0. However, scenario 1, where the decline in background mortality is slowest relative to the other two components creates a pattern of increasing variation at nearly all ages except the very youngest.

Because of its greater capacity to replicate the empirical pattern of diverging lifespan variability trends, the Siler model was used in the subsequent analysis to examine the sensitivity of the age-specific variability measures to actual changes in each parameter over time.

B Maximum likelihood estimation

For a given life table cohort (real or synthetic, as in period life tables), we denote the number of survivors to exact age x by $l(x)$, and the number of deaths between exact ages x and $x + 1$ as $d(x)$. The hazard of dying at age x, $\mu(x)$, was defined according to the Gompertz or Siler hazard equations ($\mu(x)$) in turn. The life table (conditional) single-year probability of death, $q(x)$, is given by:

$$q(x)=1-e^{-\int_x^{x+1}\mu(s)\,ds}, \quad (25)$$

and was estimated via the common approximation (Chiang 1984):

$$q(x)=1-e^{-\mu(x)}. \quad (26)$$

Note that this estimator of $q(x)$ is most reliable when the hazard can be assumed to be constant over the one-year interval.

To construct a closed form likelihood function for our life table data, we assumed that life table deaths followed a binomial distribution with $l(x)$ trials, of which $d(x)$ are failures and $l(x) - d(x)$ are successes. We treated $q(x)$ as the underlying parameter representing the probability of death. Since, as shown above, $q(x)$ is a function of the hazard $\mu(x)$, either the two parameters of the Gompertz model (α and β) or the five parameters of the Siler model (α_1, β_1, α_2, β_2, and α_3) were defined in relation to $q(x)$ and estimated via the following likelihood function:

$$\mathscr{L}(q(x)|\boldsymbol{X})=\begin{pmatrix} l(x) \\ d(x) \end{pmatrix} q(x)^{d(x)}(1-q(x))^{l(x)-d(x)}, \quad (27)$$

where $\boldsymbol{X} = (d(x), l(x))$ is the vector of observed data in life tables for Swedish females in the 111 years between 1900–2010.

Since the log likelihood function — which converts the repeated multiplication to repeated addition — reaches a maximum at the same point as the original function, we maximized the sum of the following log likelihood:

$$Log\mathscr{L}(q(x)|\boldsymbol{X})=d(x)log(q(x))+(l(x)-d(x))\,log(1-q(x)) \quad (28)$$

The chosen estimates for the model parameters were the set of numerical solutions produced when all partial derivatives of the log likelihood were set equal to zero. All parameters were estimated simultaneously, given the observed data and using the statistical software program R, and specifically the optimx package developed by Nash and Varadhan (2011). We ran the optimization procedure independently for each of the 111 period life tables, obtaining two or five simultaneous parameter estimates (depending on the model) for each life table and examining the resulting trends. Values from the 1900 period life table were used as the

baseline trajectories in the simulations, while the full series of 111 period life tables from 1900–2010 were used to estimate the parameters examined via perturbation analysis.

The procedure is sensitive to the choice of starting parameter values, and we assigned values based on parameters used by Goldstein and Wachter (2006) to characterize the mortality trajectory of European populations in the twentieth century. Starting values for the Gompertz model were $\alpha = -10$ and $\beta = 0.1$, and starting values for the Siler model were $a_1 = -2.4$, $\beta_1 = 0.9$, $a_2 = -11.6$, $\beta_2 = 0.1$, and $a_3 = -4.6$. To assure convergence of the estimates, we allowed up to 20,000 iterations and 50,000 function evaluations, with a gradient tolerance level of 0.00005.

To characterize the variability of these estimates, we calculated the Hessian matrix (the matrix of second partial derivatives of the log likelihood), took the negative expectation of this matrix to obtain the “information matrix,” and inverted the latter to obtain estimates of the variances and covariances of the maximum likelihood parameter estimates. To obtain the standard errors (i.e. the standard deviation of the sampling distribution) for each parameter estimate, we computed the square root of the diagonal elements of the final matrix. These results are available upon request.

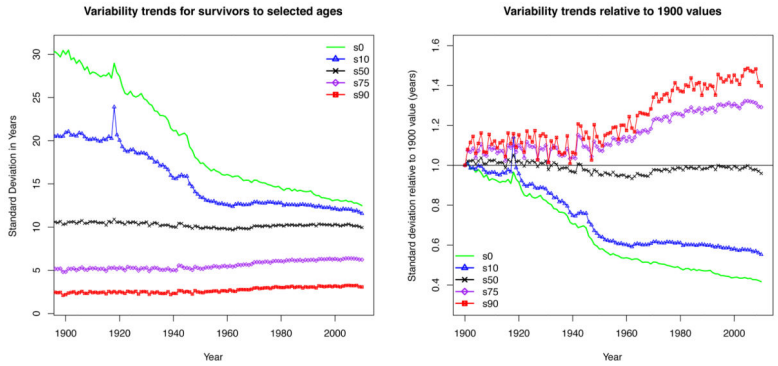

Figure 1. Trends in lifespan variation for Swedish Females, 1900–2010

Notes: Left: Trends in standard deviations of lifespan distributions for Swedish females: full population (s_0) and survivors to ages 10 (s_{10}), 50 (s_{50}), 75 (s_{75}), and 90 (s_{90}).

Right: Trends in standard deviations of lifespan distributions at the same ages relative to their values in 1900. Both perspectives show reduced variability in lifespan distributions containing younger people, but growing lifespan variability among survivors to older ages.

Source: Human Mortality Database, 2012.

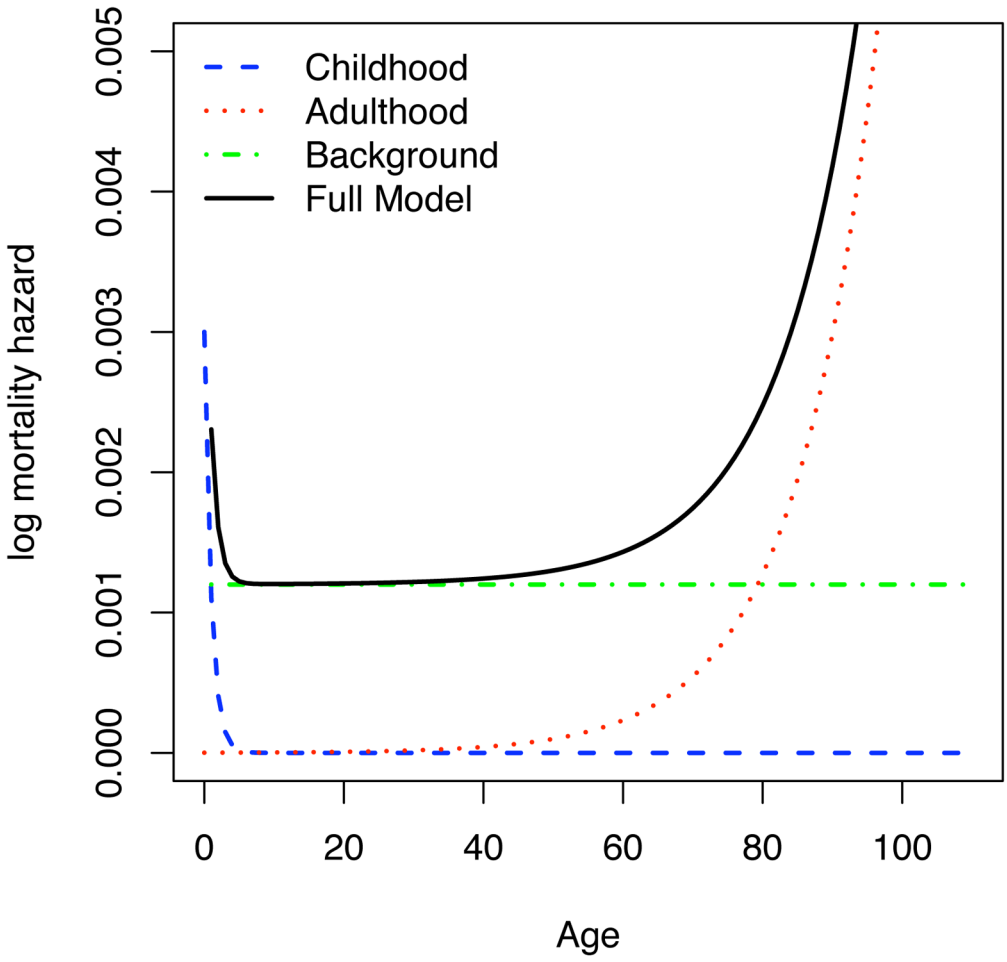

Figure 2. The three-component Siler model

Notes: $\mu(x) = e^{\alpha 1 - \beta 1 x} + e^{\alpha 2 + \beta 2 x} + e^{\alpha 3}$, where the first term on the right represents the mortality pattern dominant in childhood, the second term represents the mortality pattern dominant in adulthood, and the third term represents a background mortality level.

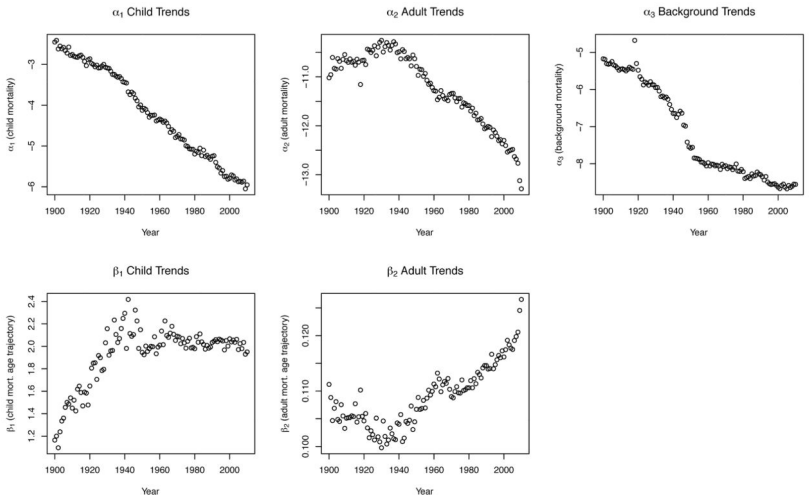

Figure 3. Trends in maximum likelihood parameter estimates for the Siler model

Notes: The child mortality parameter β_1 is negative in the Siler equation, while all other parameters are positive. Based on life tables for Swedish females 1900–2010.

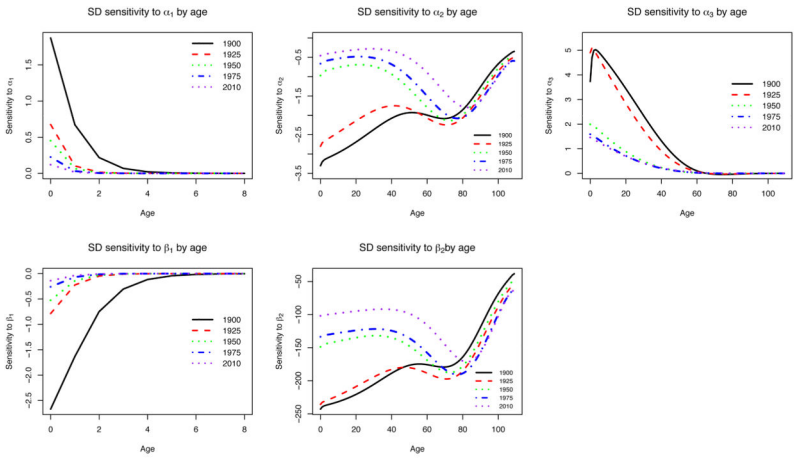

Figure 4. Sensitivity of each age-specific (conditional) standard deviation in the distribution of lifespans to unit changes in Siler model parameters for selected years

Notes: Sensitivity is measured in the same units as the standard deviation.

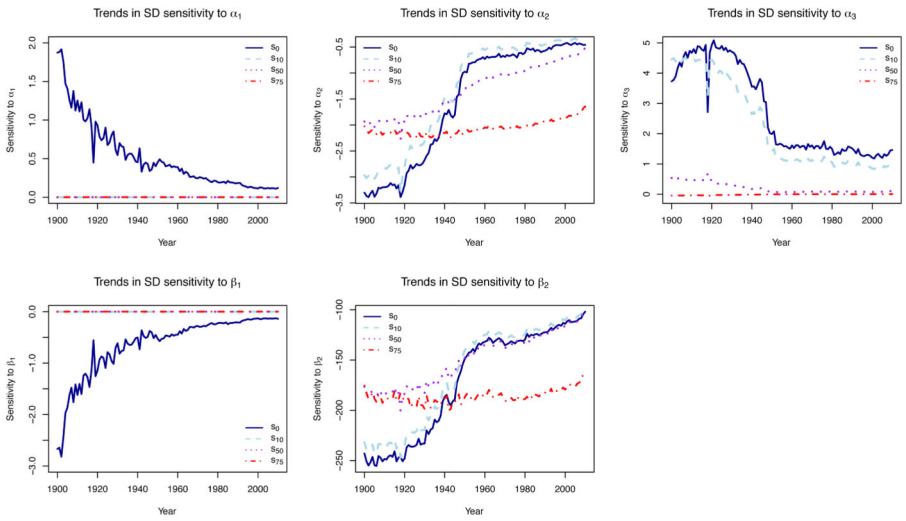

Figure 5. Sensitivity of each age-specific (conditional) standard deviation in the distribution of lifespans to unit changes in Siler model parameters for selected ages

Notes: Sensitivity is measured in the same units as the standard deviation.

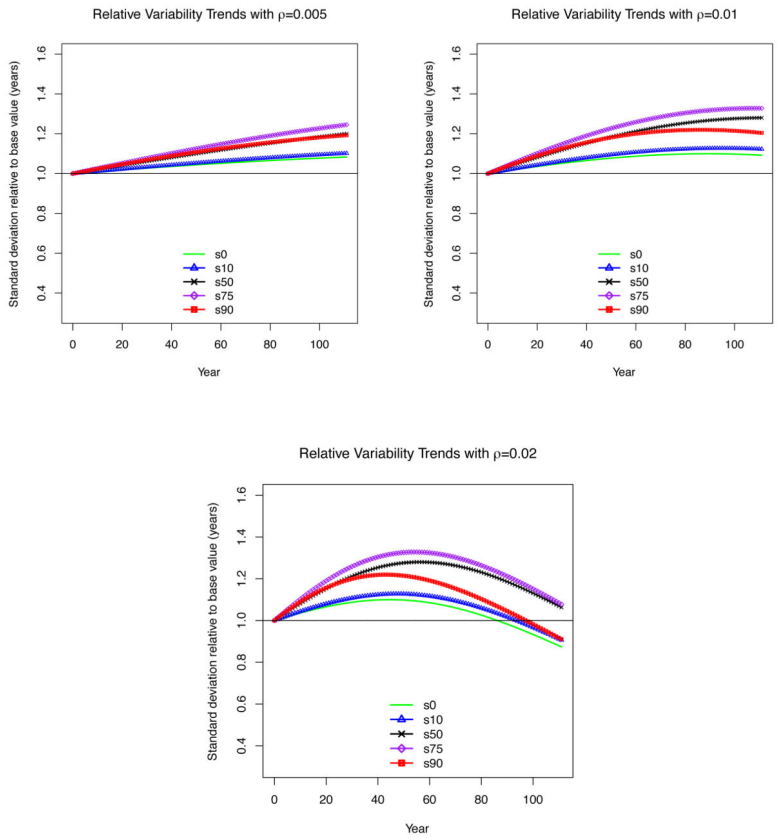

Figure 6. Simulated lifespan variability trends for 111 years based on a Gompertz model

Notes: Starting parameters are estimated from a life table for Swedish females, 1900, and age-specific mortality hazards change according to a constant annual rate (ρ).

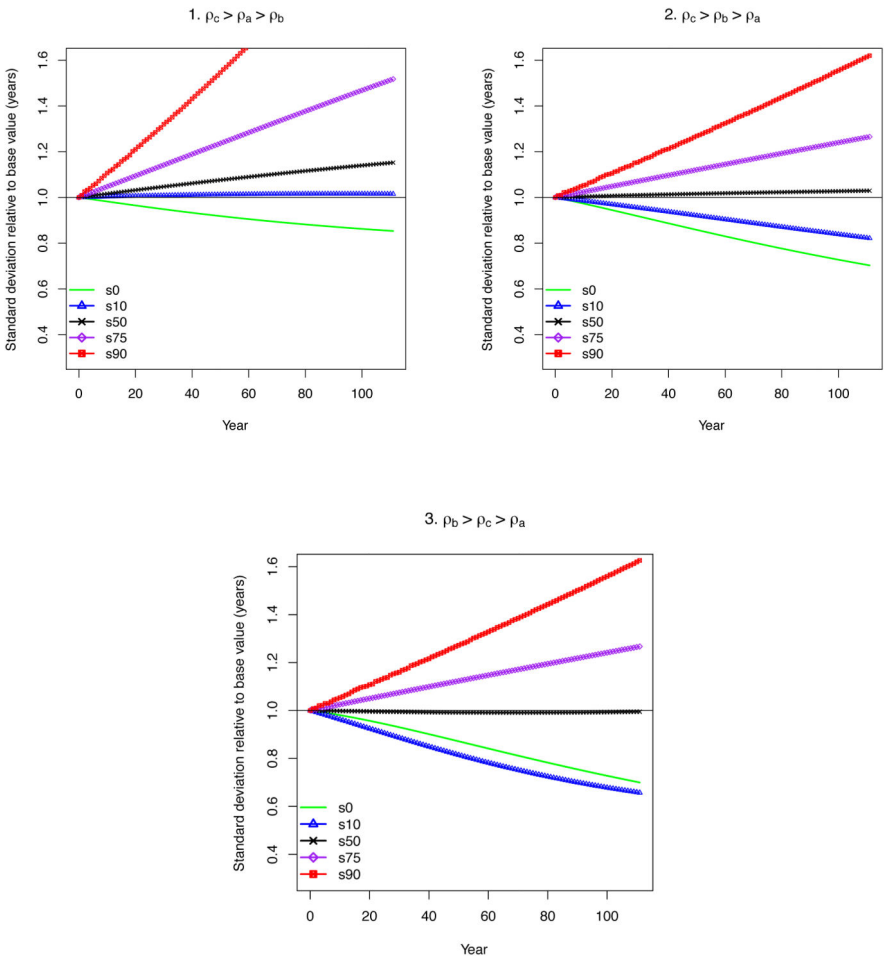

Figure 7. Simulated lifespan variability trends for 111 years based on a Siler model

Notes: Starting parameters are estimated from a life table for Swedish females, 1900. The scenarios depicted are those where the rate of childhood mortality change (ρ_c) is faster than the rate of change in adult mortality (ρ_a) and the rate of change in background mortality (ρ_b) is slowest (1), intermediate (2), or fastest (3).